1D Gas Temperature Measurements by O₂ Resonantly Ionized Photoemission Thermometry in a Mach 4 Ludwieg Tube

Walker McCord¹, Alek Clark², and Zhili Zhang^{5,*}

Dept. of Mechanical, Aerospace, and Biomedical Engineering, University of Tennessee, Knoxville, TN 37996, USA

Shelby Ledbetter³, and Mark Gragston⁴

The University of Tennessee Space Institute, Tullahoma, TN, 37388, USA

In this work, one-dimensional (1D) Oxygen-based Resonantly Ionized Photoelectron Thermometry (O_2 RIPT) technique is used for temperature measurements in a $M_\infty=4$ flow. O_2 RIPT resonantly ionizes O_2 molecules via (2+1) Resonant Enhanced Multiphoton Ionization (REMPI) process; subsequent ionization via electron impacted avalanche ionization of molecular nitrogen produces fluorescence emissions from the first negative band of N_2 through photoemission deexcitation. The fluorescence emissions of the N_2 first negative band occur at Δv_0 , 390nm; Δv_2 , 425nm; Δv_1 , 430nm and are captured by a gated intensified scientific and used for temperature determination via a Boltzmann plot based on the direct relationship with the two-photon line strength. O_2 RIPT is used to characterize the free stream static temperature across a 50.8 mm (2") line, which is compared to isentropic calculations for the Mach 4 flow. Additionally, the thermal field associated with strong compression through a normal shock generated by a blunt 25.4 mm (1") diameter cylinder is measured.

I. Nomenclature

K = Kelvin nm = nanometers mm = millimeters

II. Introduction

Off-body gas phase temperature measurements are often desirable for characterize the flow around models in high-speed wind tunnel testing. Some current non-intrusive optical thermometry techniques used to study heating around blunt bodies include Planar-Laser Induced Fluorescence (PLIF), Tunable-Diode Laser Absorption Spectroscopy (TDLAS), and Coherent Anti-stokes Raman Scattering (CARS) [1-5]. PLIF must employ the use of a tracer molecule such as Nitric Oxide or an aromatic molecule, which can alter the flow chemistry and can result in nonreal flow

¹ Aeronautical Engineer, Senior, Lockheed Martin Aeronautics Company, Marietta, Georgia, AIAA Young Professional Member.

² Graduate Student, Dept. of Mechanical, Aerospace, and Biomedical Engineering, University of Tennessee, AIAA student member

³ Graduate Student, Dept. of Mechanical, Aerospace, and Biomedical Engineering, University of Tennessee, AIAA student member.

⁴ Assistant Professor, Department of Mechanical, Aerospace, and Biomedical Engineering, and AIAA Member

⁵ Professor, Dept. of Mechanical, Aerospace, and Biomedical Engineering, University of Tennessee, AIAA Associate Fellow.

features and behavior [6-8]. TDLAS is path-integrated and limited to point measurements, making it difficult to isolate acquired data to within the test vehicle region [9-11]. A relatively new technique, oxygen-based Resonantly Ionized photoemission thermometry (O₂ RIPT), is capable of resolving gas vibrational temperature across a onedimensional (1D) line within low-enthalpy, high-speed flows without the need for particulate or gas seeding. O₂ RIPT builds upon advances in Resonant Enhanced Multi-Photon Ionization (REMPI) to resonantly excite oxygen molecules inducing electron impacted excitation of locally available nitrogen molecules, generating N2⁺. The technique is enabled through the proven assumption that the photoemissions strength within the first negative band of nitrogen, i.e., $N_2^+(B^2\Sigma_u^+ - X^2\Sigma_g^+)$, are directly related to the two-photon transitional line strength of the selectively excited absorption peak within oxygen's $O_2(X^3\Sigma(v'=0)) \to C^3\Pi(v=2)$ absorption band that lies between 285 to 289 nm. Fundamentally, the technique works by assuming that the selectively chosen peaks within the resonant absorption bands, which are temperature sensitive, can be directly represented by the excited molecular nitrogen's photoemissions of the first band. Thus, the photoemissions indirectly are representative of the rotational state distribution of the oxygen molecule. By probing multiple resonant absorption lines a statistically weighted (Boltzmann) distribution can be applied to the emission signals, enabling a temperature determination. Furthermore, since the generated photoemissions result from electron impacted excitation processes of nitrogen from oxygen, the temperature is associated with the vibrational state. The REMPI structure of O₂ and details of the underlying physics for the O₂ RIPT signal generation are have been previously described in detail and thus will not be covered here [12-14]. The curious reader is directed to a previously conducted calibration study that examined multiple parameters of the generated photoemission signal and its capacity for assigning gas temperatures through O₂ RIPT [15].

As part of this work, O₂ RIPT is demonstrated for off-body gas temperature measurements around a cylinder in Mach 4 flow. A fundamental design challenge associated with hypersonic vehicles is the reduction of aerodynamic heating imparted to the vehicle. At high-supersonic and especially hypersonic speeds, bodies are typically blunt nosed to an extent in order to reduce the heat transfer rates to manageable proportions and to allow for internal heat conduction. Depending on the relative bluntness at the nose of the flight vehicle and the speed at which it is traveling, a strong detached bow shock or normal shock will develop. This detached shock converts most of the kinetic energy associated with high flight velocities to thermal and chemical energy. This conversion of energy creates a high temperature region directly aft of the shock and while this region is associated with high total stagnation heating, the detached shock reduces imparted heating to the aerothermal structure by dissipating the thermal energy into the surrounding air via shock wave compression with the remaining heating arising within the boundary layer [16]. Furthermore, the detached shock represents a trade-off between thermal management and aerodynamic efficiency, as the strong entropy change through the shock will result in high surface pressures on the body resulting in an increase in the aerodynamic drag [17]. However, the reduced surface heating accomplished from detached shocks makes the tradeoff worthwhile, and there are ways to mitigate the negative impact of aerodynamic efficiency (i.e., aerospikes, forward mass injection, and freestream energy deposition) [18-22]. Since the maximum local heat transfer rate in most cases will occur in the vicinity of this forward stagnation point, the fluid interactions and flow dynamics within this region have been of considerable interest in the research community. Because of the strong falling pressure gradients and large heat transfer to the surface, the boundary layer within this region can be expected to be laminar [23]. However, relative to flight velocity, the thermal and chemical energy within this area is sufficiently strong enough to dissociate oxygen and nitrogen molecules resulting in non-equilibrium flow and real gas effects, making it a challenging area for CFD simulations to model accurately [24]. Thus, it is critically important to obtain experimental measurements that can provide dependable benchmark validation data.

III. Experimental Setup

A. Mach 4 Wind Tunnel

The University of Tennessee Space Institute (UTSI) Mach 4 Ludwieg tube located within the Tennessee Aerothermodynamics Laboratory (TALon) was utilized for conducting the O_2 RIPT experiments. The facility, shown in Fig. 1 [25, 26], has a 61 by 61-centimeter (24 by 24 inch) nozzle exit area and a 1.82-meter test-section length. The total run time of is approximately 200 milliseconds, of which about 130 milliseconds is steady state flow conditions. The nominal total pressure and total temperature for these tests were 439.7 kPa and 295 K respectively and air was used as the test gas. Using the isentropic relations, the static pressure and temperature were determined to be approximately 2.890 kPa and 70.2 K respectively. The freestream per length Reynolds number was 21.2×10^6 m⁻¹.

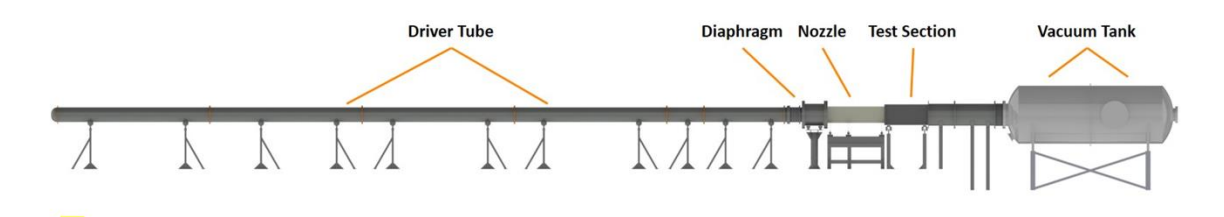


Figure 1: The UTSI Mach 4 Ludwieg tube.

B. Optical Setup

The second harmonic of an injection seeded Nd:YAG laser (Spectra Physics Quanta Ray Pro 290) with a pulse width of 8ns, repetition rate of 10 Hz, with average lasing energy of 1 Joule per pulse was used to pump a dye laser (Sirah Precision Scan) that utilized a mixture of Rhodamine 590 and Rhodamine 610 to produce lasing light around 574 nm (0.02 cm⁻¹ linewidth). The dye laser was frequency doubled to generate deep ultraviolet (UV) light around 287 nm for probing the $O_2(X^3\Sigma(v'=0) \to C^3\Pi(v=2))$ resonant absorption band of oxygen. Nominal pulse energies of approximately 30 mJ/pulse were measured at the output of the frequency doubling unit over the range of 285 nm to 288 nm.

The beam was steered vertically using a UV fused silica right-angle prism and focused using a fused silica plano-convex lens of f=500 mm focal length. The focusing distance of the lens was selected that allowed the beam to pass through the fused silica windows in the tunnel floor unimpeded and to achieve the high-intensity needed for multiphoton absorption in the region near the center of the tunnel test-section. The generated O_2 RIPT signal was imaged using a f=1000mm camera lens and an intensified scientific camera (PI-MAX4 1024f) with a sensor size of 1024 pixels by 1024 pixels. A square (50 mm x 50 mm) Schott's® glass BG3 filter of 1 mm thickness was used to remove laser scattering and other background light contributions from the signal. Visualizations of the full setup within the TALon lab are shown in Fig. 2.

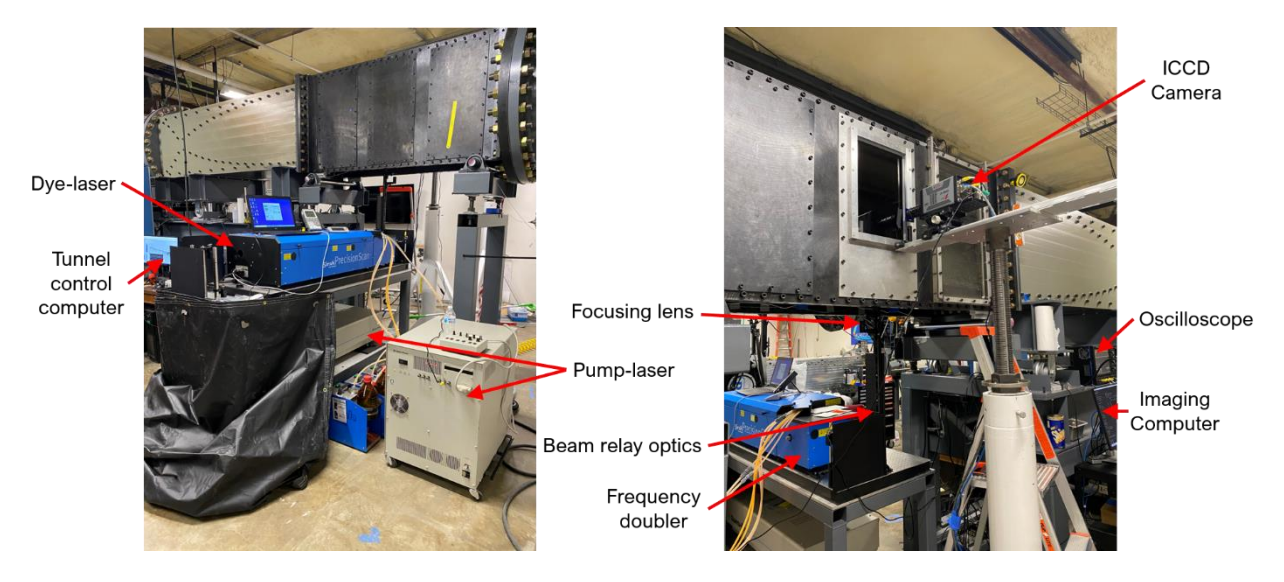


Figure 1: O₂ RIPT setup for the Mach 4 tunnel.

C. Model

In addition to measuring the tunnel freestream static temperature, the temperature field near a circular cylinder model was also measured. Models of this nature are used to generate strong bow shocks and temperature increases for studying stagnation heating and real gas effects in hypersonic flows. The dissipation of strong viscous interactions and flow mixing behind the detached shockwave generates a high-temperature region behind the detached shockwave.

The strong temperature gradient from freestream to behind shock generated presented an excellent opportunity to examine O₂ RIPT's ability for resolving the large thermal gradient associated with flow through a strong shockwave. The cylinder model consisted of a 25.4 mm diameter 3D printed (Formlabs 3L) cylinder that was 10.16 cm in length. The model was mounted on a 0.7 m long rod which allowed it to be translated either upstream or downstream of the tunnel for precise alignment with the laser beam. Black photography tape was used to minimize laser reflections on the model. the cylinder was positioned vertically, as shown in Fig. 3, to allow the O₂ RIPT line to be generated along the length of the model behind the detached shock. This configuration and layout will allow for probing the vibrational temperature along most of the model's length.

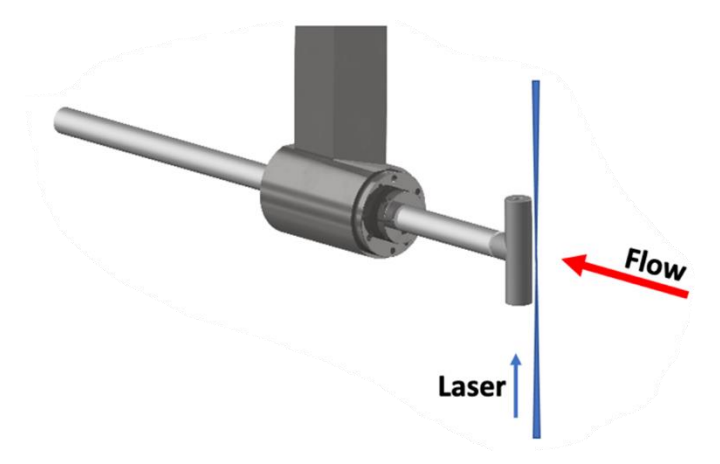


Figure 2: Cylindrical model in the vertical orientation and (b) the horizontal orientation. The beam enters the tunnel from the bottom and flow is from right to left in this view.

IV. Results and Discussion

A. Mach 4 Freestream

One-dimensional oxygen-based RIPT measurements using only direct imaging of photoemissions generated from $N_2^+(B^2\Sigma_u^+ - X^2\Sigma_g^+)$ first negative band were acquired to measure the freestream static temperature across an approximately 5 cm line length. Four wavelengths were selected for this measurement, which were chosen based on previous low-temperature calibration work [15]. At each wavelength, an O_2 RIPT line was generated by focusing the laser using a 300 mm plano-convex lens, this allowed positioning of the line within the test-section such that effects from the wall boundary layer were avoided. Due to steady state tunnel run time and laser repetition rate, only two RIPT signals were acquired for each wavelength during each tunnel firing. The pre-run image along with the RIPT signal image at 287.33 nm is shown by Fig. 4.

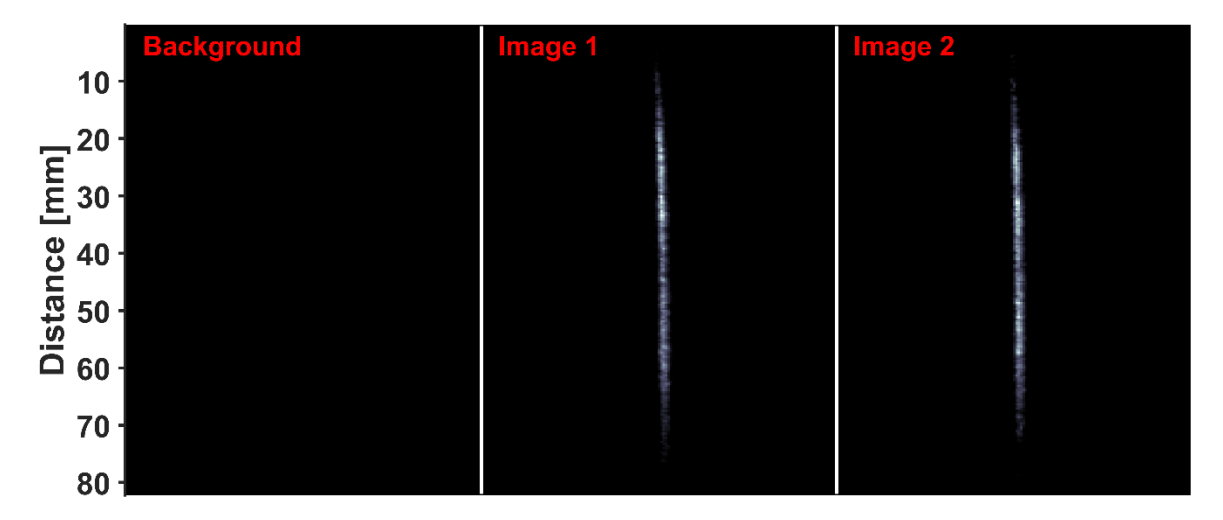


Figure 3: Images showing the O₂ RIPT emissions from 287.33 nm laser excitation in a Mach 4 freestream as collected from one run of the Mach 4 tunnel.

Previous studies of signal-pressure dependence within a closed environment found that as pressure decreases from atmospheric, the signal emission strength is drastically reduced until it is indistinguishable from background noise around 41.4 kPa (6 Psia) [27]. However, it was found that even with a tunnel freestream static pressure of approximately 2.89 kPa (0.41 Psia) for these tests, the high flow velocity coupled with cold static temperature enabled strong photoemission generation. Additionally, the lower temperature and pressure in the Mach 4 flow reduce the quenching, which boosts the signal. These effects coupled to enable signal generation that was stronger than previous signals recorded at standard temperature and pressure conditions within a closed environment.

The emissions were post-processed using the same technique and equations discussed in previous work [15, 27] to relate the photoemission strength to the vibrational temperature. The resulting O_2 RIPT temperature measurement of the free stream across a 52 mm line length is shown in Fig. 5. The average free stream temperature as measured by O_2 RIPT was approximately 75.7 K with mean fluctuations of approximately ± 1 K. These fluctuations are largely due to limited data used to calculate the temperatures; specifically, a single shot at each wavelength. Isentropic flow theory is used to compare and validate the O_2 RIPT measurement. Considering the isentropic relations, the static-to-total temperature ratio is $T/T_0 = 0.238$. Thus, the theoretical freestream static temperature is approximately 70.2 Kelvin. If the ± 3 K error associated error of the O_2 RIPT technique is considered, then the experimental values show good agreement with the expected temperature values.

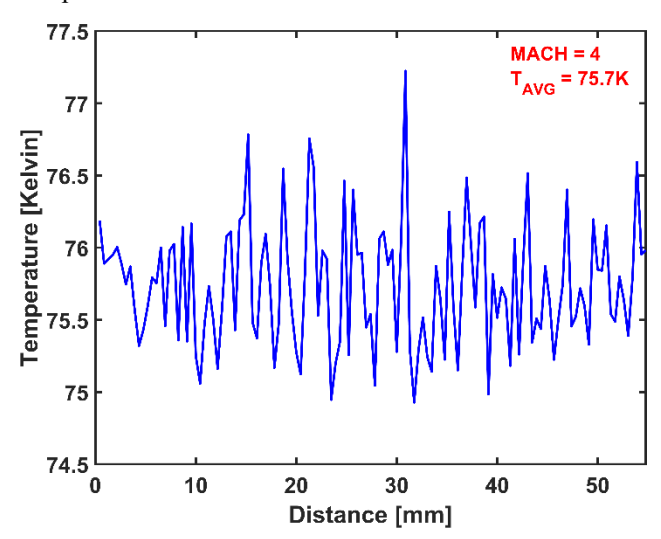


Figure 4: O₂ RIPT line temperature measurement of the tunnel freestream.

B. Vertically Oriented Cylindrical Model

With O2 RIPT successfully demonstrated in the free stream flow, the cylinder model was installed for measurements in the shock layer. For the vertically oriented model, the laser beam was directed along the axis of the cylinder model with a 3 mm offset from the windward face of the cylinder. The focus of the beam was centered across the vertical extent of the model. It was necessary to offset the beam from the model as the tunnel slightly moves during operation. To provide a better understanding of the flow field and estimating shock standoff distance, Schlieren imaging and computations were done prior to testing. Schlieren images were acquired at 50 kHz rates to examine the shock stability and characterize stand-off distance. An instantaneous schlieren image of the model in the Mach 4 flow is shown in Fig. 6. From the schlieren image, it was found that the shock stand-off distance at the centerline of the model is approximately 6.4 mm from the model surface.

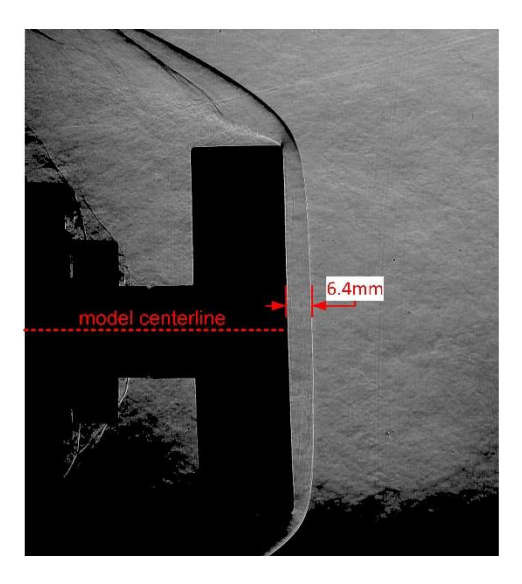


Figure 5: A schlieren image of the vertically oriented cylinder model. The shock standoff distance was determined to the 6.4 mm for these conditions. The slight angle of the model in the schlieren imaging is due to a subtle 3D printing error, but had no significant impact on the flow.

The computations of the model flow-field were done using ANSYS Fluent. The RANS simulations used the Spalart-Allmaras turbulence model and were done with varying mesh sizes to ensure sufficient convergence. The initialization parameters were based on the tunnel static conditions and velocity. The results for the Mach number and static temperature fields are shown in Fig. 7. The shock standoff distance according to the CFD was approximately 7.2 mm.

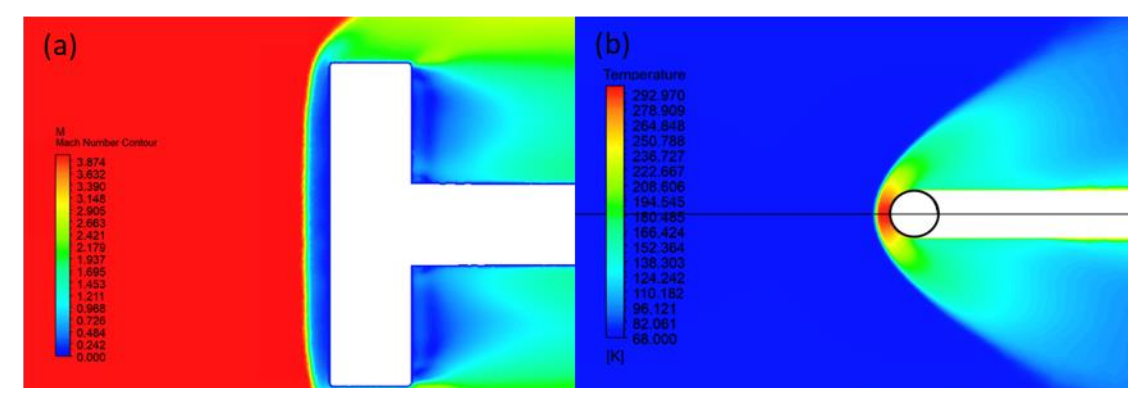


Figure 6: CFD of cylinder model showing (a) Mach contours, and (b) the temperature contours along planes of symmetry.

Figure 8(a) shows an experimentally collected raw image of the RIPT signal and with the model location artificially added to the image to aid in line stand-off distance visualization. As shown in the CFD, the flow should be nearly stagnant in the shock layer and recover nearly all of the total temperature. The O_2 RIPT measurement provided an average temperature of 296.5 ± 5.93 K across a one-inch line, which is depicted in Fig. 8(b). The average experimental value is then in good agreement with expectations. Furthermore, since the difference between experimental and expected values are almost identical to that of the free stream measurement; perhaps suggesting that the tunnel free stream temperature is slightly higher than the theoretical value.

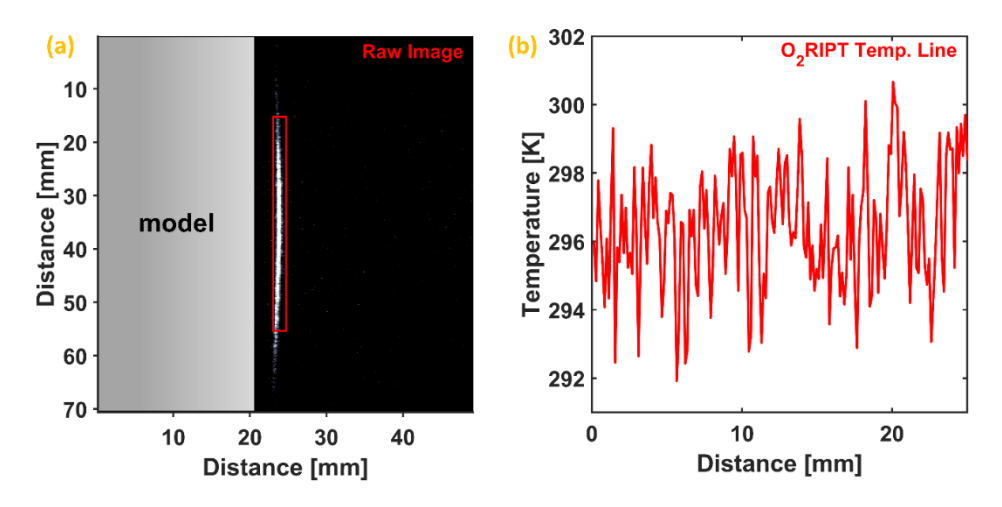


Figure 7: Image of model and O₂ RIPT line (a), and O₂ RIPT temperature measurement behind shock (b).

V. Conclusion

In summary, Oxygen-based Resonantly Ionized Photoemission Thermometry has been demonstrated for one-dimensional line temperature measurements of up to approximately 5.2 cm in length in a Mach 4 wind tunnel environment. First, the free stream temperature within the test section was characterized over a 5.2 cm long O₂ RIPT line. Since the tunnel is non-heated and low-enthalpy, the theoretical static temperature (approximately 70.2 Kelvin), was well outside the calibration range that O₂ RIPT had been demonstrated previously [15, 27, 28]. Furthermore, the O₂ RIPT measurement determined an average gas vibrational temperature across the 5.2 cm line of approximately 75.7±3 K, which is in relatively good agreement with the theoretical considerations from the isentropic flow relations given the error margin. This work then provides supporting evidence that the calibration wavelengths previously determined for the cold-gas temperatures (<293 Kelvin) [15] are widely applicable; maintaining relevant population distributions for accurate temperature assignments far outside the lowest calibration setpoint.

Additionally, a cylinder model that generated a strong detached shock and induces flow phenomena that is relevant to shockwave compression heating was studied. The measurement in the shock layer with the beam aligned with the axis of the cylinder gave a fairly uniform temperature with an average value of 296.5 ± 5.93 K. The measurements with the beam aligned perpendicular to the cylinder axis clearly show a resolved thermal gradient in the shock layer and across the bow show. Together, these results demonstrate the capability of O_2 RIPT for off-body gas thermometry in high-speed flows.

VI. Acknowledgements

This work is supported by University of Tennessee, NSF- 2026242 and DOE.

VII. References

- 1. Miller, V. A., Gamba, M., Mungal, M. G., and Hanson, R. K. "Single-and dual-band collection toluene PLIF thermometry in supersonic flows," *Experiments in fluids* Vol. 54, No. 6, 2013, pp. 1-13.
- 2. Danehy, P., Wilkes, J. A., Alderfer, D. W., Jones, S. B., Robbins, A., Patry, D., and Schwartz, R. "Planar laser-induced fluorescence (PLIF) investigation of hypersonic flowfields in a Mach 10 wind tunnel," *25th AIAA Aerodynamic Measurement Technology and Ground Testing Conference*. 2006, p. 3442.
- 3. Steelant, J., Langener, T., Hannemann, K., Marini, M., Serre, L., Bouchez, M., and Falempin, F. "Conceptual design of the high-speed propelled experimental flight test vehicle HEXAFLY," 20th AIAA international space planes and hypersonic systems and technologies conference. 2015, p. 3539.
- 4. Dolvin, D. "Hypersonic international flight research and experimentation (HIFiRE) fundamental science and technology development strategy," *15th AIAA International Space Planes and Hypersonic Systems and Technologies Conference*. 2008, p. 2581.
- 5. Cutler, A. D., Cantu, L. M., Gallo, E. C., Baurle, R., Danehy, P. M., Rockwell, R., Goyne, C., and McDaniel, J. "Nonequilibrium supersonic freestream studied using coherent anti-Stokes Raman spectroscopy," *AIAA Journal* Vol. 53, No. 9, 2015, pp. 2762-2770.
- 6. Abram, C., Fond, B., and Beyrau, F. "Temperature measurement techniques for gas and liquid flows using thermographic phosphor tracer particles," *Progress in energy and combustion science* Vol. 64, 2018, pp. 93-156.
- 7. Gross, K., McKenzie, R., and Logan, P. "Measurements of temperature, density, pressure, and their fluctuations in supersonic turbulence using laser-induced fluorescence," *Experiments in Fluids* Vol. 5, No. 6, 1987, pp. 372-380.
- 8. Jiang, N., Webster, M., Lempert, W. R., Miller, J. D., Meyer, T. R., Ivey, C. B., and Danehy, P. M. "MHz-rate nitric oxide planar laser-induced fluorescence imaging in a Mach 10 hypersonic wind tunnel," *Applied Optics* Vol. 50, No. 4, 2011, pp. A20-A28.
- 9. Chang, L. S., Strand, C. L., Jeffries, J. B., Hanson, R. K., Diskin, G. S., Gaffney, R. L., and Capriotti, D. P. "Supersonic mass-flux measurements via tunable diode laser absorption and nonuniform flow modeling," *AIAA journal* Vol. 49, No. 12, 2011, pp. 2783-2791.
- 10. Farooq, A., Jeffries, J. B., and Hanson, R. K. "In situ combustion measurements of H2O and temperature near 2.5 μm using tunable diode laser absorption," *Measurement Science and Technology* Vol. 19, No. 7, 2008, p. 075604.
- 11. Zhou, X., Liu, X., Jeffries, J. B., and Hanson, R. "Development of a sensor for temperature and water concentration in combustion gases using a single tunable diode laser," *Measurement Science and Technology* Vol. 14, No. 8, 2003, p. 1459.
- Wu, Y., Sawyer, J., Zhang, Z., and Adams, S. F. "Flame temperature measurements by radar resonance-enhanced multiphoton ionization of molecular oxygen," *Applied optics* Vol. 51, No. 28, 2012, pp. 6864-6869.
- 13. Wu, Y., Zhang, Z., and Adams, S. F. "Temperature sensitivity of molecular oxygen resonant-enhanced multiphoton ionization spectra involving the C 3Π g intermediate state," *Applied Physics B* Vol. 122, No. 5, 2016, pp. 1-10.
- 14. Wu, Y., Zhang, Z., and Ombrello, T. M. "Spatially resolved measurement of singlet delta oxygen by radar resonance-enhanced multiphoton ionization," *Optics letters* Vol. 38, No. 13, 2013, pp. 2286-2288.
- 15. McCord, W., Clark, A., and Zhang, Z. "One-dimensional air temperature measurements by air resonance enhanced multiphoton Ionization thermometry (ART)," *Optics Express* Vol. 30, No. 11, 2022, pp. 18539-18551.

- 16. Eggers, A. J., Allen, H. J., and Neice, S. E. A comparative analysis of the performance of long-range hypervelocity vehicles: National Advisory Committee for Aeronautics. 1957.
- 17. Mehta, R. "Numerical heat transfer study around a spiked blunt-nose body at Mach 6," *Heat and Mass Transfer* Vol. 49, No. 4, 2013, pp. 485-496.
- 18. Marley, C. D., and Riggins, D. W. "Numerical study of novel drag reduction techniques for hypersonic blunt bodies," *AIAA journal* Vol. 49, No. 9, 2011, pp. 1871-1882.
- 19. Zhong, K., Yan, C., Chen, S.-s., Zhang, T.-x., and Lou, S. "Aerodisk effects on drag reduction for hypersonic blunt body with an ellipsoid nose," *Aerospace science and technology* Vol. 86, 2019, pp. 599-612.
- 20. Riggins, D., Nelson, H. F., and Johnson, E. "Blunt-body wave drag reduction using focused energy deposition," *AIAA journal* Vol. 37, No. 4, 1999, pp. 460-467.
- Alexander, S. R. "Results of Tests of determine the Effect of a Conical Windshield on the Drag of a Bluff Body at Supersonic Speeds." National Aeronautics and Space Administration Hampton Va Langley Research Center, 1947.
- 22. Gerdroodbary, M. B., Imani, M., and Ganji, D. "Investigation of film cooling on nose cone by a forward facing array of micro-jets in hypersonic flow," *International Communications in Heat and Mass Transfer* Vol. 64, 2015, pp. 42-49.
- 23. Lees, L. "Laminar heat transfer over blunt-nosed bodies at hypersonic flight speeds," *Journal of Jet Propulsion* Vol. 26, No. 4, 1956, pp. 259-269.
- 24. Schmidt, D. P., Gopalakrishnan, S., and Jasak, H. "Multi-dimensional simulation of thermal non-equilibrium channel flow," *International journal of multiphase flow* Vol. 36, No. 4, 2010, pp. 284-292.
- 25. Gragston, M., and Smith, C. D. "10 kHz molecular tagging velocimetry in a Mach 4 air flow with acetone vapor seeding," *Experiments in Fluids* Vol. 63, No. 5, 2022, pp. 1-9.
- 26. Kreth, P. A., Gragston, M., Davenport, K., and Schmisseur, J. D. "Design and initial characterization of the UTSI Mach 4 Ludwieg tube," *AIAA Scitech 2021 Forum*. 2021, p. 0384.
- 27. McCord, W., Gragston, M., Plemmons, D., and Zhang, Z. "O 2 based resonantly ionized photoemission thermometry analysis of supersonic flows," *Optics Express* Vol. 30, No. 22, 2022, pp. 40557-40568.
- 28. Dogariu, A., Dogariu, L. E., Smith, M. S., Lafferty, J., and Miles, R. B. "Single shot temperature measurements using coherent anti-Stokes Raman scattering in Mach 14 flow at the Hypervelocity AEDC Tunnel 9," *AIAA Scitech 2019 Forum.* 2019, p. 1089.